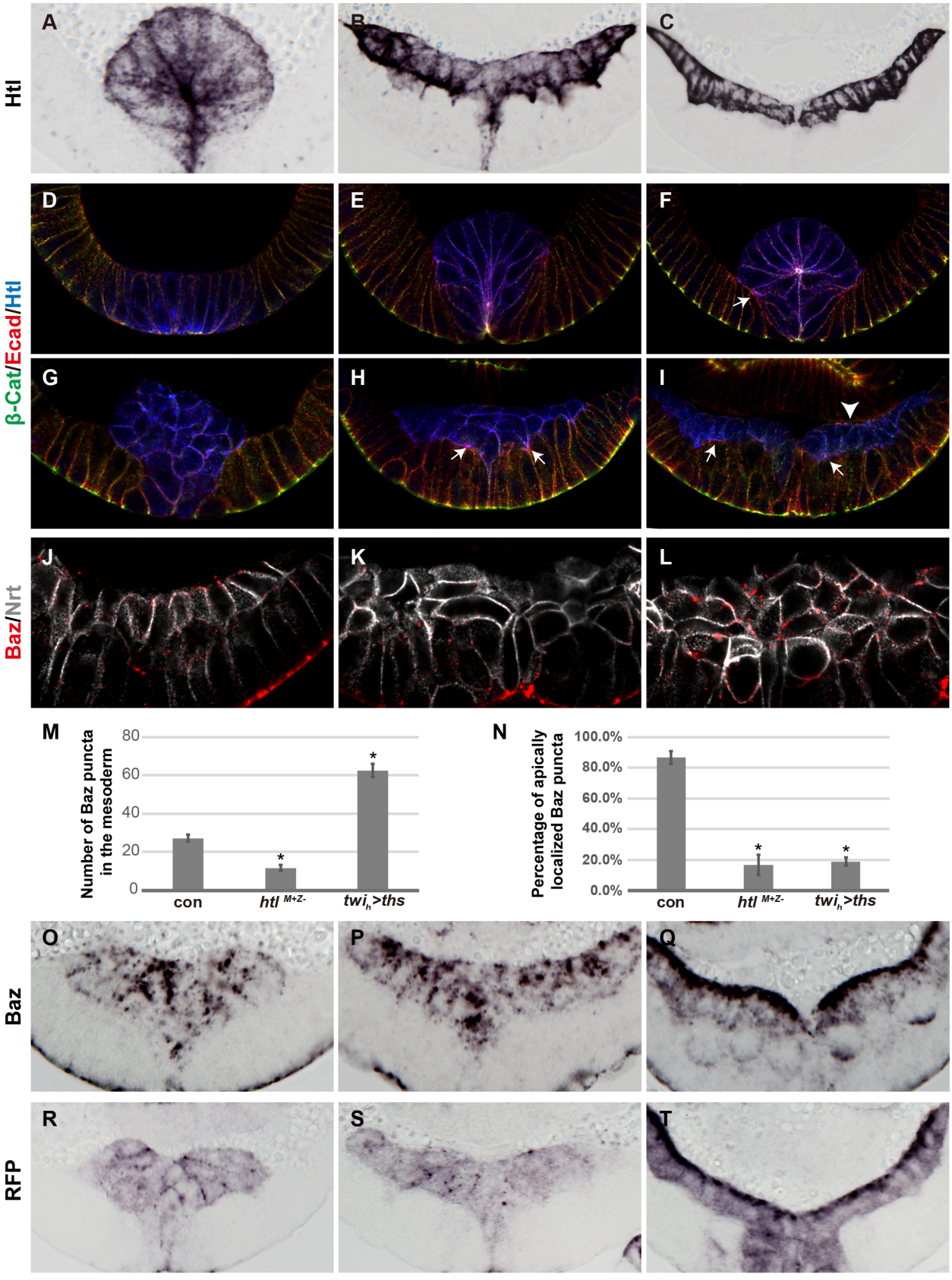

Supplementary Figure 1. Localization of Htl, AJ protein E-Cad, β-Cat and fluorescent protein-tagged Baz with alternative antibodies.

(A-C) Immunostaining of embryos carrying a *htl-mcherry* transgene at stage 7 (A), stage 9 (B), or stage 10 (C) using an anti-RFP antibody.

(D-I) Colocalization using anti-β-Cat (green), anti-E-Cad (red) and anti-Htl (blue) in embryos of stage 6 (D), stage 7 early (E), stage 7 late (F), stage 8 early (G), stage 8 late, and stage 9 (I).

(J-L) Baz (red) fluorescent immunostaining in stage 10 control (J), *htl* $^{M+Z-}$ (K) and *twi$_h$-pyr* (L) embryos. Embryos were co-stained with Nrt (light grey) to visualize the cellular morphology. Confocal single scans shown were taken from manually cross-sectioned embryos.

(M-N) Quantification of Baz expression in J-L. Total number of Baz puncta in the mesoderm is significantly decreased in *htl* $^{M+Z-}$ mutants, but increased in *twi$_h$>ths* embryos compared to the control (asterisks, M, $p<0.001$). Percentage of apically localized Baz puncta is decreased in both mutants (asterisks, N, $p<0.001$). Numbers of embryos for each genetic background at stage 10 are as following (total number of the confocal scans is indicated inside the parenthesis): control: 3(5); *htl*$^{M+Z-}$: 3(3); *twi$_h$>ths*: 7(7). Confocal scans were taken under the same setting. Baz puncta were counted with the same threshold in Image J. Student *t*-test was used to test significance. Error bars represent s.d.

(O-Q) Immunostaining of embryos expressing *baz-GFP* driven by *twi$_h$-GAL4* with anti-Baz antibody at stage 8 early (O), stage 8 late (P), and stage 10 (Q).

(R-T) Immunostaining of embryos expressing *baz-RFP* by the same driver, with anti-RFP antibody at stage 8 early (R), stage 8 late (S), and stage 9/10 (T).

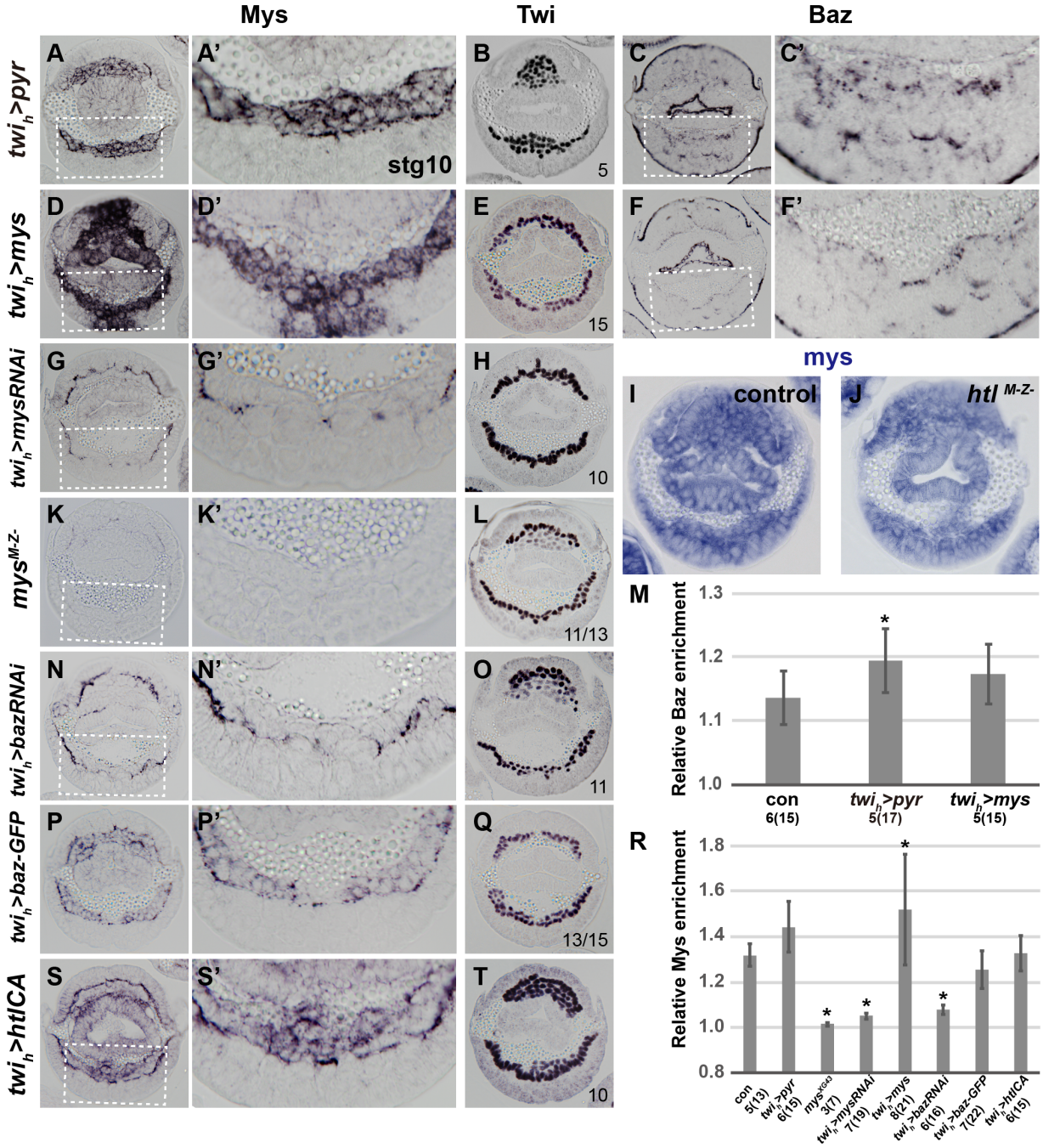

Supplementary Figure 2. Mys and Baz levels in the mesoderm are regulated by FGF. **(A-H,K,L,N-Q,S,T)** Stage 10 embryos of the indicated genotypes immunostained using antibodies against Mys (A,D,G,K,N,P,S and magnified views of boxed regions in A',D',G',K',N',P',S'), Twi (B,E,H,L,O,Q,T) or Baz (C,F and magnified views of boxed regions in C',F'). Number of st10 embryos analyzed by Twi antibody staining is indicated at the bottom right corner in B, E, H, L, O, Q and T. Ratios, if given, represent percentage showing phenotype.

(I, J) Expression of *mys* transcripts detected by in situ hybridization using a riboprobe in control and htl^{M-Z-} mutant embryos around stage 9. *mys* expression is identified in the ectoderm, mesoderm as well as endoderm.
(M) Quantification of relative Baz enrichment in the mesoderm in C' and F' compared to the control (see Fig 4A,B).
(R) Quantification of relative Mys enrichment in the mesoderm-ectoderm interface in A', D', G', K', N', P', S' compared to the control (see Fig 5A',Q).
Number of embryos used for statistical analysis is indicated underneath the genotype with the number of sections inside the parenthesis. Error bars represent s.d. Asterisks represent datapoints that are significantly different from the control based on student *t*-test ($p<0.05$).

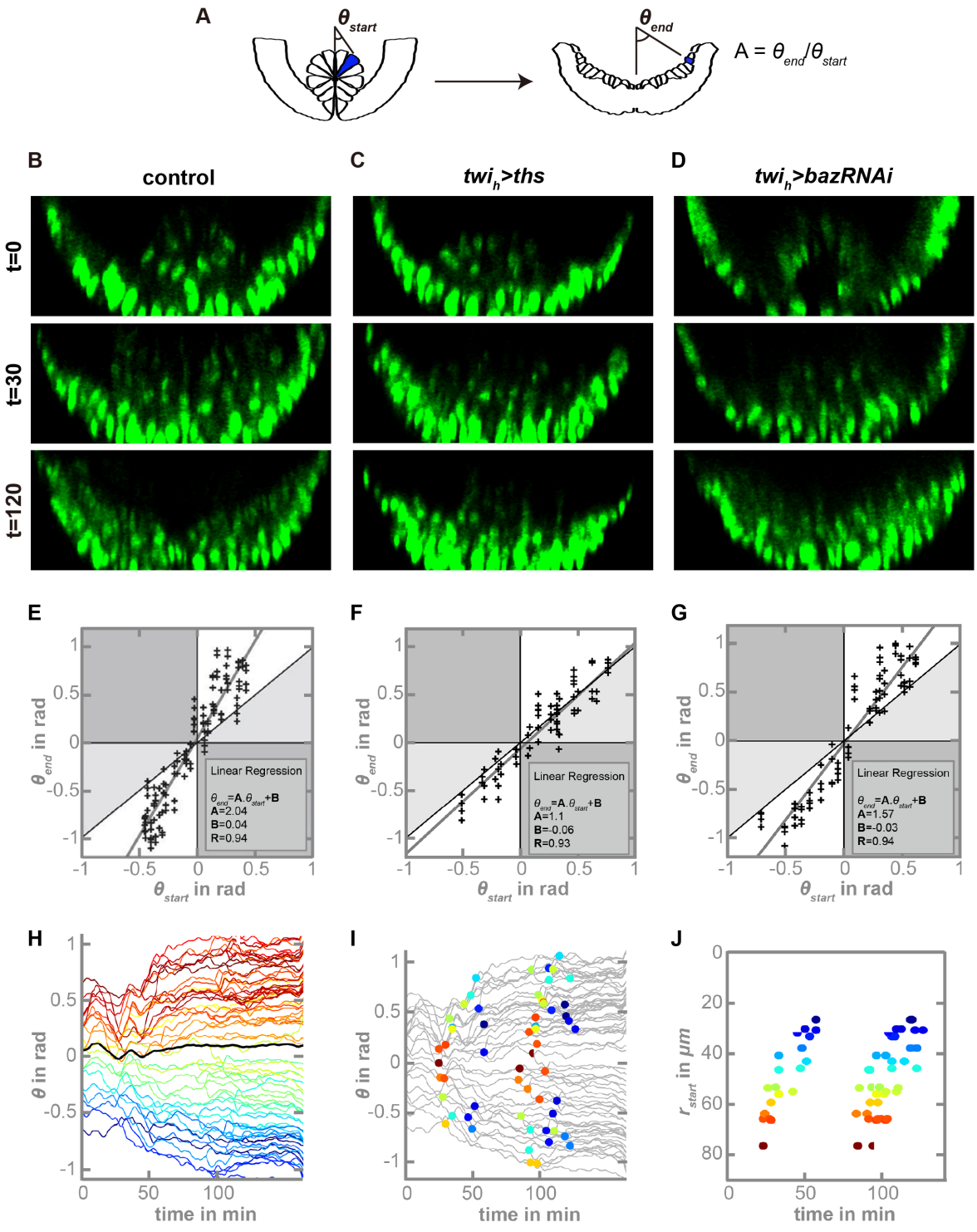

Supplementary Figure 3. Calculation of the mesoderm spreading profile in control, *twi$_h$>ths* and *twi$_h$>baz RNAi* mutant embryos.

(A) Schematic showing how azimuthal angular position changes upon normal spreading movement of cells.

(B-D) Representative stills at the indicated times from movies of embryos of control (B: twi-Gal4 x *yw*), ectopically expressing Ths ligand in the mesoderm (C: twi_h-Gal4 x UAS.ths) and knocking down *baz* in the mesoderm (D: twi_h-Gal4 x UAS.*baz*.RNAi) that also contain the H2A-GFP transgene, which allows visualization of mesoderm cells throughout the course of their migration by live in vivo imaging.
(E-G) Plots of azimuthal angular position, θ_{start} *vs.* θ_{end}, for tracked mesoderm cells in (B), (C) and (D). In control embryo, the slope of the line, A, is close to 2 and has been previously used to define the degree of collective movement of mesoderm cells (McMahon et al., 2008). Upon ectopic expression of Ths, A is reduced to 1 (F), demonstrating that cells do not spread as θ_{start} is equivalent to θ_{end}. In a less severe *twi_h>baz RNAi* embryo that has been tracked (G), A falls between 1 and 2 (θ_{end} is less than twice θ_{start}, as found in the control), suggesting spreading is compromised without Baz participation.
(H-J) See supplemental movie 4. Tracking analysis of the *twi_h>baz RNAi* embryo with a mild spreading phenotype (D,G) displayed in a similar manner to the control (Figure 7F,I,L).

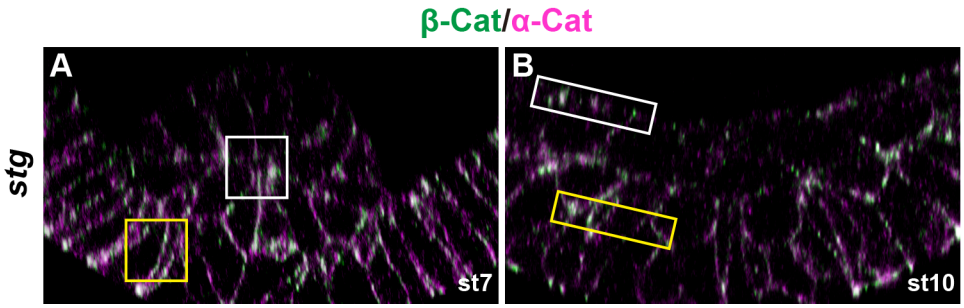

Supplementary Figure 4. Example of calculating the enrichment of colocalized α-Catenin and β-Catenin in the mesoderm. Z-projections from confocal scans of *stg* embryos co-stained by antibodies against α-Catenin (violet) and β-Catenin (green) at stage7 (A) and stage10 (B). Boxes in white indicate the mesoderm signal while boxes in yellow of the same size indicate the ectoderm signal. Gray value measurements were taken for both in Image J. The relative enrichment was calculated by dividing the value in white box by the value in yellow box.

SUPPLEMENTAL MOVIES

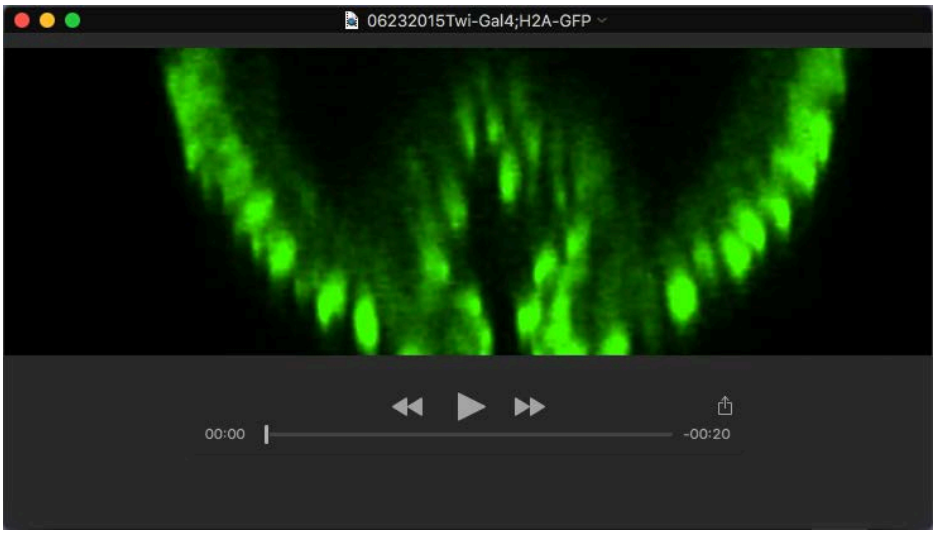

Movie 1 shows mesoderm cell spreading in an embryo containing an H2A-GFP transgene that allows tracking of cell movement in *yw* background.

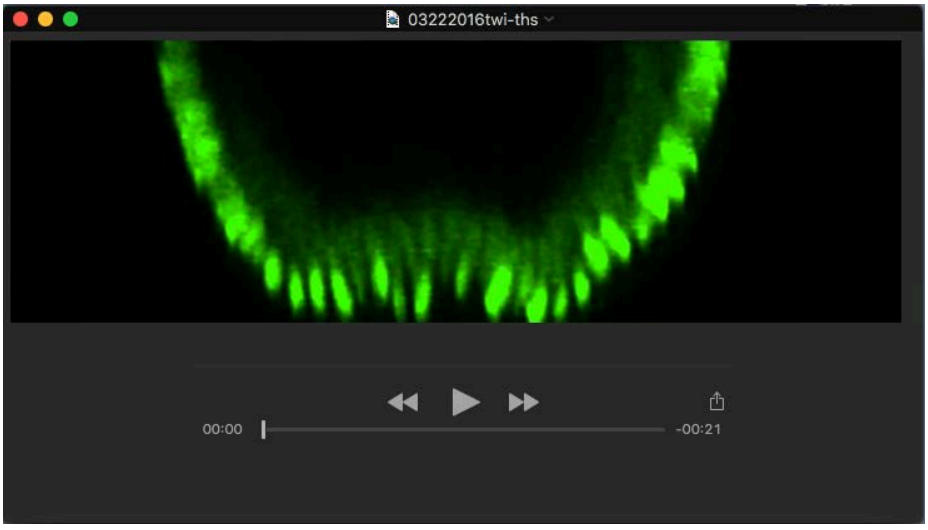

Movie 2 shows mesoderm cell spreading in a *twi$_h$>ths* mutant embryo containing the H2A-GFP transgene.

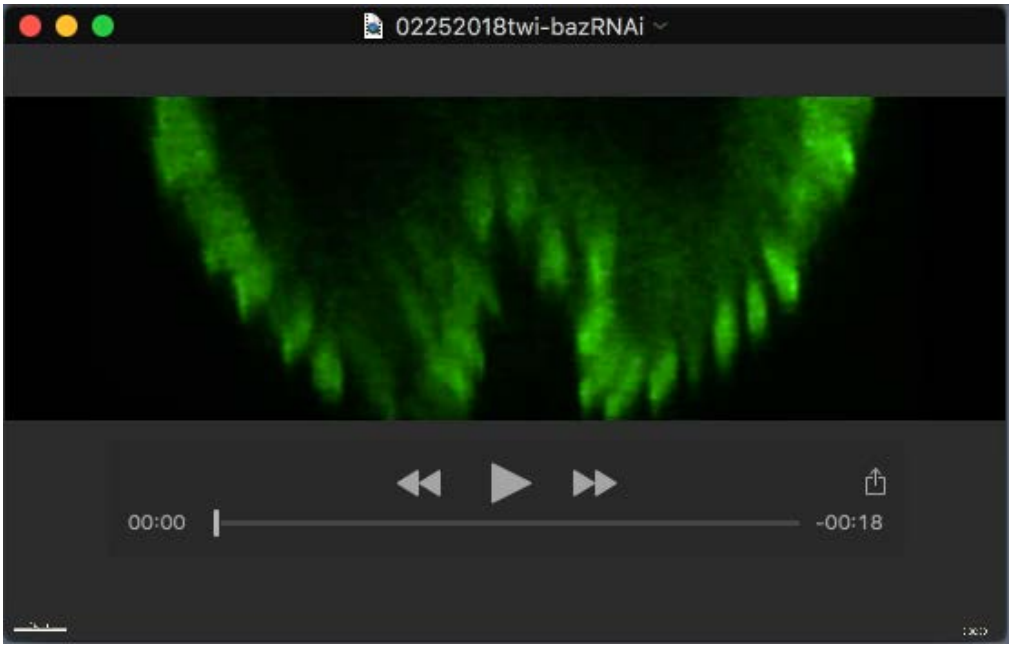

Movie 3 shows mesoderm cell spreading in *twi$_h$>baz RNAi* mutant background, carrying H2A-GFP transgene, that exhibits defects as early as invagination (likely "strong" phenotype)..

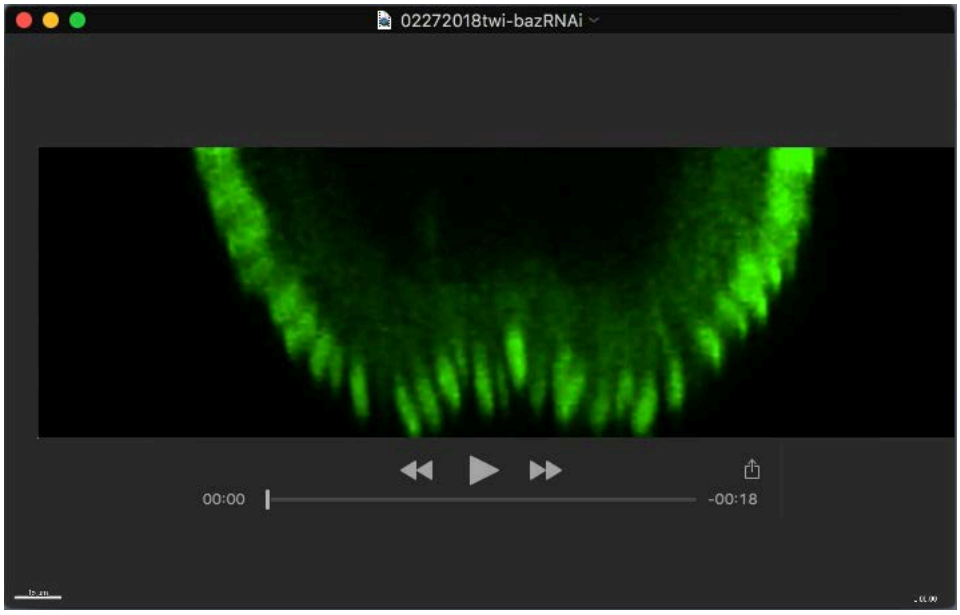

Movie 4 shows mesoderm cell spreading in an H2A-GFP transgenic embryo in *twi$_h$>baz RNAi* mutant background that exhibits normal invagination but mild spreading defect later (likely "mild" phenotype).